JGR Biogeosciences

RESEARCH ARTICLE
10.1029/2022JG006786

Key Points:

- Riverine total particulate phosphorus (TPP) in stormflow was more than doubled while the increased soil erosion decreased the TPP:SPM ratio
- The fresh-brackish water interface moved downstream, causing sediment resuspension, adding extra TPP flux and buffering DIP concentration
- Increasing labile phosphorus fluxes through the estuary with a high TDN:TDP ratio are likely contributory factors to coastal eutrophication

Supporting Information:

Supporting Information may be found in the online version of this article.

Correspondence to:

N. Chen,
nwchen@xmu.edu.cn

Citation:

Zhang, M., Krom, M. D., Lin, J., Cheng, P., & Chen, N. (2022). Effects of a storm on the transformation and export of phosphorus through a subtropical river-turbid estuary continuum revealed by continuous observation. *Journal of Geophysical Research: Biogeosciences*, *127*, e2022JG006786. https://doi.org/10.1029/2022JG006786

Received 2 JAN 2022
Accepted 25 JUL 2022

Author Contributions:

Conceptualization: Nengwang Chen
Data curation: Mingzhen Zhang, Jingjie Lin
Formal analysis: Mingzhen Zhang
Funding acquisition: Nengwang Chen
Project Administration: Nengwang Chen
Software: Peng Cheng
Writing – original draft: Mingzhen Zhang
Writing – review & editing: Michael D. Krom, Jingjie Lin, Nengwang Chen

Effects of a Storm on the Transformation and Export of Phosphorus Through a Subtropical River-Turbid Estuary Continuum Revealed by Continuous Observation

Mingzhen Zhang[1,2], Michael D. Krom[3,4], Jingjie Lin[1,2], Peng Cheng[2], and Nengwang Chen[1,2]

[1]Fujian Provincial Key Laboratory for Coastal Ecology and Environmental Studies, College of the Environment and Ecology, Xiamen University, Xiamen, China, [2]State Key Laboratory of Marine Environment Science, Xiamen University, Xiamen, China, [3]Morris Kahn Marine Station, Charney School of Marine Sciences, University of Haifa, Haifa, Israel, [4]School of Earth and Environment, University of Leeds, Leeds, UK

Abstract Major storms, which are increasing in frequency due to climate change, flush pollutant nutrients, including phosphorus (P), from river catchments through estuaries to the coast. Changes in P speciation alter the potential for P removal in sediments. We measured suspended particle matter (SPM), dissolved and particulate phosphorus and other physicochemical parameters at two river outlets of the Jiulong River (SE China) and a fixed station in the estuary during an entire storm (June 2019). During the storm, riverine total particulate phosphorus (TPP) more than doubled to approximately 100 μg P L^{-1} mainly from pollutant sources, while increased soil erosion reduced the TPP:SPM ratio by 1/3. The riverine DIP increase during the storm was only moderate (approximately 25%). As the storm intensified, the fresh-brackish water interface moved downstream. There was increased SPM and TPP flux (up to approximately 25,000 kg P d^{-1}) from resuspended surficial sediment that had been deposited during normal flow in the adjacent tidal flats and mangrove areas. These sediments had acted as microbial incubators. Reduced Fe in the resuspended sediment was converted to labile Fe oxyhydroxides in the oxic water column, which adsorbed DIP (and probably also DOP) and increased labile TPP exported downstream. During the storm, the total flux of riverine dissolved nutrients increased while the TDN:TDP ratio decreased from 43:1 to 32:1. Our study showed that estuaries are locations for temporary deposition of labile TPP during normal flow, which are flushed out during major storms, likely resulting in increased eutrophication, including encouraging harmful algal blooms in coastal zones.

Plain Language Summary An important effect of climate change is the increase in intensity and frequency of major storms. Such storms flush pollutants including Phosphorus (P) which is often the nutrient which limits the amount of algal growth, from river catchments, through estuaries to the sea. Here, we measured dissolved and suspended P and relevant other physical and chemical data at the outlet of two branches of the Juilong river in SE China and a station in mid-estuary during an entire storm in June 2019. We found that during the storm pollutant P (particularly that attached to particles) was flushed out of the river into the estuary. As the storm intensified, the boundary of the river-estuary moved downstream. The increased water flow in the upper estuary resuspended pollutant-rich sediment which had been deposited during periods of low flow. This sediment included a chemical form of Fe which removed dissolved P from the water but increased the amount of labile particulate P passing through the estuary. We conclude that major storms increase the flux of pollutant P to the coast likely causing increased eutrophication including harmful plankton blooms.

1. Introduction

A known effect of global climate change is an increase in both the frequency and intensity of storms (Annamalai & Liu, 2005; Rozemeijer et al., 2021). The increased rainfall and discharge associated with storm events increase the riverine suspended particulate matter (SPM), particulate and dissolved nutrient flux to the estuary and hence to coastal areas, causing changes in water quality throughout its passage to the sea (Castagno et al., 2018; De Carlo et al., 2007). Phosphorus (P), as a key nutrient, plays an essential role in aquatic biological production (Hu et al., 2021; Reinhard et al., 2017). Excess phosphorus inputs will cause eutrophication in many waterbodies, especially those with P limitation. Although unpolluted estuaries and coastal marine systems are generally considered limited by nitrogen (Ryther, 1954), many recent studies have found P limitation to increase as a result of high N:P in anthropogenic inputs in many riverine catchments and from atmospheric inputs (Canela

et al., 2020; Elser et al., 2009; Nelson, 2000). In China, many important estuaries and bays are now P-limited, such as the Yellow River estuary (Pan et al., 2013), the Yangtze Estuary (Wu et al., 2020), and the Pearl River Estuary (Xu et al., 2008), and are relevant to this particular study, Xiamen Bay (Chen et al., 2021). Therefore, it is important to study how increased storm flows affect the speciation and flux of P from rivers through estuaries to coastal areas.

The nature and flux of phosphorus in almost all major rivers worldwide are dominated by anthropogenic sources and human-altered physical and biogeochemical processes (Maavara et al., 2015; Powers et al., 2016), especially in areas of high population density, such as Southeast Asia (Seitzinger et al., 2010). The Jiulong River in southeast China is a subtropical river where there is mixed land use with nonpoint phosphorus sources, including agricultural activities such as fertilizer application, together with animal or human wastes in rural areas, as well as point sources, which are mainly sewage outlets from wastewater treatment plants and intensive animal cultivation (Huang & Hong, 2010; Huang et al., 2019). During normal flow conditions, biogeochemical processes alter phosphorus speciation after it reaches the river channel (Yuan et al., 2021). For example, dissolved inorganic phosphorus (DIP) can be adsorbed onto inorganic particles and/or taken up by biological uptake. The resultant particulate P can be deposited at least temporarily in river channels and particularly in cascade reservoirs (Maavara et al., 2015). During storm events, both phosphorus sources and processes in river channels are altered, resulting in a substantial increase in phosphorus flux down the river (Chen et al., 2013, 2015). However, our knowledge of the changes in P speciation during storms exiting river catchments into estuaries is still incomplete (Bowes et al., 2005; Li et al., 2017; Yang et al., 2021).

Estuaries are important biogeochemical filters and locations that transform riverine nutrients and particles, modifying their nature and fluxes to coastal waters. Under normal flow conditions, the estuarine turbidity maximum zone (ETM) is an important location for biogeochemical transformations, particularly for P and N species (Burchard et al., 2018; Chen et al., 2018; Garnier et al., 2010; Lin et al., 2022; Yu et al., 2020). SPM interacts with dissolved nutrients in the water column via processes such as adsorption and desorption, as well as many microbial processes such as nitrification and denitrification (Asmala et al., 2017; Lin et al., 2022; Yu et al., 2020). In addition, during normal flow, particulate matter containing excess P is deposited in the upper estuary and adjacent mudflats (Conley et al., 1995; Slomp, 2011). Early diagenesis and mineralization of biogenic organic matter occurs in these upper sediments, and labile organic and iron-bound phosphorus is transformed into DIP, which is released into pore water (Fernandes & Nayak, 2009; Krom & Berner, 1981). However, during storms, sediment erosion caused by increased water flow can resuspend these poorly consolidated sediments, releasing and transforming P species in the water column (Niemisto & Lund-Hansen, 2019). DIP can be fixed by labile iron oxide and/or clay minerals in the suspended particles in the oxic water column (Conley et al., 1995; Froelich, 1988; Pan et al., 2017). Understanding how phosphorus is exported from the upper estuary during storm events is necessary to develop science-based management strategies for controlling eutrophication in estuaries and adjacent coastal regions.

In recent years, river-estuary-coast continuum systems have been considered as a whole both in scientific studies and integrated management from a holistic perspective (Hong et al., 2015; Xenopoulos et al., 2017). Freshwater river plumes rich in pollutant nutrients, particularly during storm periods, form one of the primary connectors between river-estuary systems and coastal oceans. They can have a major impact on coastal ecosystems, causing increased eutrophication and sometimes harmful algal blooms (HABs) (Chen et al., 2021). However, few studies have carried out synchronous observations to capture the systematic changes of SPM and nutrients through the period of increasing and decreasing discharge in the exits from the river(s) and adjacent estuary, which is necessary to increase the understanding of the impact of storms on the river-estuary-coast continuum.

In this study, we carried out a detailed study of the effects of a major storm on the sources, transformation and export of phosphorus species from a subtropical river to the adjacent estuary (the Jiulong River-estuary continuum system) in southeast China. Intensive sampling was carried out at the two river outlets of the Jiulong River and at a station in the upper estuary, which is the center of the ETM zone in the Jiulong River Estuary, during normal flow. Freshwater discharge and concentrations of SPM and dissolved and particulate phosphorus species were measured to determine the nature and flux of P species out of the river catchment and through the estuary during the storm. This study aimed to understand the relative contributions from rivers and adjacent wetlands during storms to identify biogeochemical transformation processes that alter the nature and flux of phosphorus species through the river-estuary system as a result of increased stormflow. In a parallel study, N species were

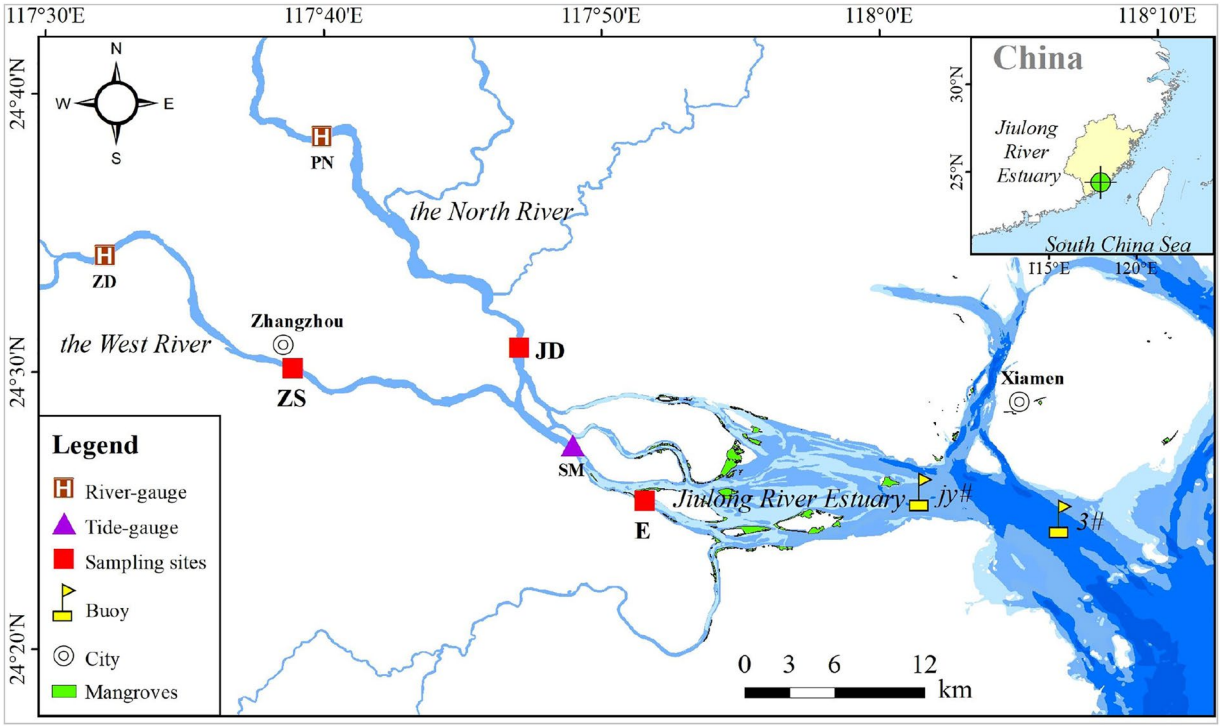

Figure 1. Map of the Jiulong River Estuary showing the fixed estuary site (Station E), two buoys (Buoy jy#, Buoy 3#), the outlets of the North River (JD) and the West River (ZS), the tide gauge site at Shima (SM) and the two river gauges in the lower river (PN and ZD). Light blue indicates shallow water.

measured at the same locations during the same storm (Lin et al., 2022), enabling TDN:TDP ratios to be calculated in the river-estuary continuum.

2. Materials and Methods

2.1. Study Area

The Jiulong River Estuary is located on the western side of the Taiwan Strait in Southeast China and receives an annual freshwater discharge of approximately 1.47×10^{10} m^3 from the upper Jiulong River, which is the second largest river in Fujian Province (Figure 1). The Jiulong River is composed of two major tributaries (the North River and the West River) with a total drainage area of 14,740 km^2, mainly flowing through the south channel of the Jiulong River Estuary into Xiamen Bay and eventually into the Taiwan Strait. The North River contributes two-thirds of the total discharge of the Jiulong River with 9,640 km^2 drainage, while the West River exports the other one-third with a drainage area of 3,940 km^2. A third tributary (the South River) flows into the Jiulong River Estuary in the middle reaches with only a small discharge. Small areas of mangroves dominated by *Kandelia obovate* are distributed along the bank of the estuary near the South River.

The surface area of the Jiulong River Estuary is approximately 100 km^2, and the water depth ranges from 3 to 16 m. The climate of this region is controlled by the subtropical monsoon climate, with an annual average temperature of 20.9°C. The mean annual rainfall is 1,772 mm, of which more than 70% occurs during the wet season from April to September. The Jiulong River Estuary is a macro tidal estuary and has a typical semidiurnal tide with an average tidal range of 3.9 m. The average hydraulic retention time of the estuary is approximately 2–3 days. It has been estimated that approximately 2.46×10^6 tons of suspended sediment per year are transported into Xiamen Bay, which is mainly from river input and sediment resuspension in the turbidity maximum zone. There are usually two turbidity maximum zones (ETMs) in the Jiulong River Estuary, one of which is located on the western side of Haimen Island in the upper-middle part (~Station E), and the other is located on the eastern side of Jiyu Island in the lower reach. Strong tidal mixing is a major controlling factor of material migration in the Jiulong River Estuary.

2.2. Sampling Campaign

Three sites were selected for storm observation (Figure 1). Station E was located between A6 and A7 (Yu et al., 2019) in the upper estuary. The other two sites were situated at the outlets of the Jiulong River above the sections of the river-estuary continuum, which were affected by tides. Site JD was located at the mouth of the North River, and ZS was located at the mouth of the West River.

The storm event in this study was the second major storm in June 2019, which was during the wet season with the longest duration from 10 June to 23 June (Figure 2a). Both the North River (NJR) and the West River (WJR) had major flood pulses from 11 June to 18 June (Figure 2b). The maximum discharge of the total river (JLR) was 2,750 $m^3 s^{-1}$ measured hourly at 6:00 on 15 June. The relatively stable river flow before the storm was 745 $m^3 s^{-1}$. According to previous research (Chen et al., 2018), baseflow and flood are the periods when the river discharge is less than and more than 1.2 times the previous flow, respectively. Therefore, the Initial and Ending periods were defined as baseflow, where the total river discharge was less than 1.2 times the previous relatively stable flow. Rising and Falling periods were defined as flood, where the river discharges were higher than 1.2 times the previous stable flow. The periods of Initial, Rising, Falling and Ending were, respectively from 10 to 9:00 on the 11, 10:00 on the 11 to 6:00 on the 15, 7:00 on the 15 to 18 and 19 to 23 (Figure 2d).

A total of 76 surface water samples were collected by a 5 L Niskin bottle water sampler approximately 0.5 m away from the riverbank throughout the storm. Two of the samples were collected in initial to represent the state before the storm. Seventeen samples were collected every 2 hr from 13:00 on 11 June to 19:00 on 12 June, when the discharge at Station E increased sharply for the first time. The remaining 57 water samples were collected every 2 hr from 7:00 to 19:00 every day until 23 June, except 18 June (one sample collected), 20 June (no samples collected) and 22 June (no samples collected). Additionally, an in-situ multiparameter sonde (Aqua TROLL 600, USA) was located 1 m above the surface sediment and used to measure environmental parameters hourly. In addition, daily samples were collected at the JD and ZS sites to represent the average concentration for the outlets of the Jiulong River on that day.

2.3. Determination of Physicochemical Parameters

All the water samples were stored in 1 L precleaned HDPE plastic bottles. Approximately 500 mL of each sample was filtrated by using pre-dried GF/F (0.7 μm) filters on site. All filters were oven-dried at 105°C for at least 18 hr before use to obtain a constant weight as the initial weight. A total of two filters were required for each water sample. The filtrates were collected in preacid-cleaned 50 mL centrifuge tubes, which were then stored in cooling containers (temperature <4°C) and transported back to the laboratory, where they were stored at 4°C in a fridge for a maximum of 1 week before dissolved nutrients were determined. The GF/F filters with particulate matter were refrigerated in the same way as the filtrates on site and then were transported to the laboratory, where they were frozen at −20°C for subsequent determination of suspended particulate matter (SPM) and particulate phosphorus species.

Bottom environmental parameters, such as salinity, turbidity, pH, DO, and temperature, were measured by an in-situ multiparameter sonde (Aqua TROLL 600, USA). Surface salinity was measured using a portable multiparameter water quality tester (WTW, Germany). Dissolved inorganic phosphorus (DIP) and dissolved inorganic nitrogen (DIN) as NO_3-N, NO_2-N, and NH_4-N in the original water samples were determined by segmented flow automated colorimetry (San++ analyzer, Germany). Total dissolved phosphorus (DTP) was determined after digestion with 4% alkaline potassium persulfate and analysis of DIP. DOP was the difference between DTP and DIP (Yuan et al., 2021). The instrument detection limit was 0.08 μmol L^{-1} for DIP, 0.10 μmol L^{-1} for NO_3-N, 0.04 μmol L^{-1} for NO_2-N, and 0.40 μmol L^{-1} for NH_4-N. The precision for measurements was calculated by repeated (duplicate) determinations of 10% of the water samples. The summed relative error of the determinations was less than 5%. To determine accuracy, a standard reference material provided by the National Environmental Protection Agency was analyzed, and the results were within ±5% of the stated standard concentrations. SPM was determined as the weight difference between predried GF/F filters and the same filters with sample after oven-drying (105°C) to constant weight. The oven-dried GF/F filter for each water sample was then combusted at 550°C in a muffle furnace for 1.5 hr and extracted with 10 mL of 1 M HCl to determine TPP as DIP. A separate GF/F filter with sample was extracted with 15 mL Milli-Q water, and a subsample (5 mL) was taken to measure adsorbed P (AP). The filter was then treated with 5 mL of 3 M HCl to a final concentration of

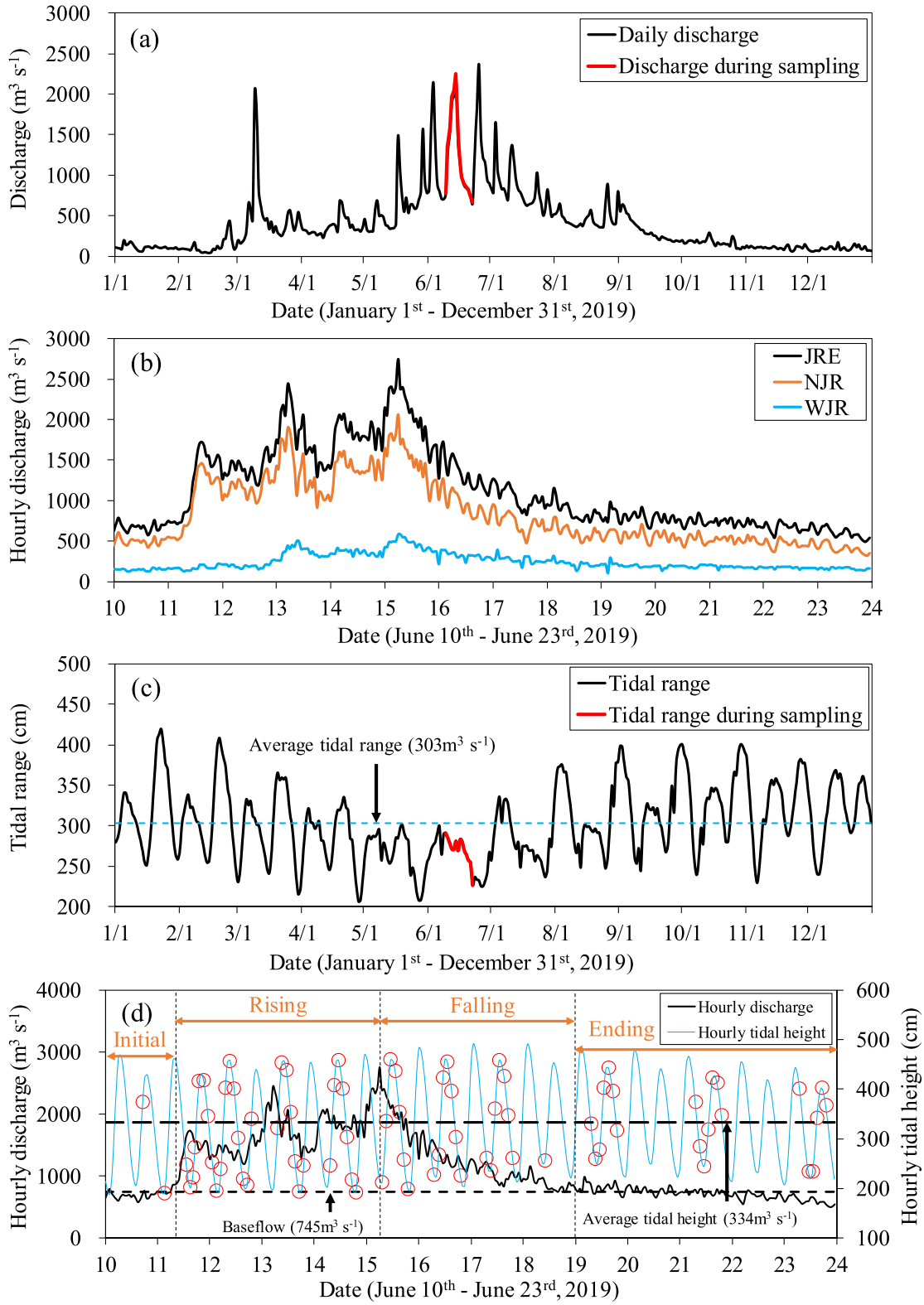

Figure 2. Hydrological and tidal characteristics of the Jiulong River Estuary during 2019 (a and c) and during the June storm observation (b and d). Figure 2a shows the combined daily discharge of NJR and WJR (Jiulong River water) to the estuary during 2019. Figure 2b shows the hourly combined daily discharge of NJR and WJR (Jiulong River water) to the estuary during the June storm period. Figure 2c shows the tidal range in the Jiulong River Estuary during 2019. Figure 2d shows the tidal range at Station E during the storm period in June 2019. The red circles in (d) indicated the time when individual samples were taken for subsequent analysis in the lab.

1 M HCl to extract and determine PIP, which was analyzed using the same procedure as that used for DIP (see above). POP was defined as the difference between TPP and the sum of AP and PIP.

2.4. Auxiliary Data and Statistical Analysis

River discharge was measured by the local government at the nearest hydrological stations in the Jiulong River Basin, in which PN was located on the NJR and ZD was located on the WJR. The discharge of the Jiulong River Estuary was the sum of water flow in the two tributaries adjusted according to the ratio of catchment area between hydrological station and Station E ($Discharge_{estuary} = Discharge_{NJR} \times 1.03 + Discharge_{WJR} \times 1.08$). Daily water discharge and daily constituent concentrations were incorporated into LOADEST software developed by USUG to calculate riverine fluxes of SPM and various phosphorus species through the adjusted maximum likelihood estimation (AMLE) method. For estuarine flux, the summed discharge of the Jiulong River Estuary and estuarine constituent concentration at low tide were applied to estimate estuarine SPM and phosphorus fluxes using the same method as that used for the river. A water residence time of approximately 1 day was estimated for storm water to flow from the river stations of sites JD for the North River and ZS for the West River to Station E in the estuary. Therefore, the estuarine time corresponding to the same flood pulse was 1 day later than the riverine time. The tidal range at Shima tide-gauge was obtained from the National Marine Data and Information Service (http://www.coi.gov.cn/).

A three-dimensional numerical model was developed in the Jiulong River Estuary to simulate the salinity of each layer at Station E during the storm event. ANOVA was performed in the SPSS program to test differences between storm periods following the Kolmogorov-Smirnov test and variance homogeneous test.

3. Results

3.1. Physical and Hydrological Conditions

The total river discharges of Initial, Rising, Falling, and Ending measured hourly were 701.2 ± 69.1, 1691.6 ± 335.6, 1245.8 ± 418.1, and 708.7 ± 92.9 $m^3\ s^{-1}$, respectively (Figure 2d). The North River (NJR) contributed 73.4 ± 5.0% of the total river runoff, considerably more than the West River (WJR), especially during the Rising period (Figure 2b). The Jiulong River Estuary (JRE) was sampled during a neap tide where the daily tidal range of the Shima gauge decreased from 291 to 226 cm, lower than the annual average (303 cm) (Figure 2c).

The surface salinity at Station E was in the range of 0–0.1‰, and the bottom salinity was from 0 to 3.4‰ (Figure 3a). The salinity in baseflow (Initial and Ending) was higher than that in flood (Rising and Falling). Bottom salinity was affected by tide during baseflow, with higher values (0.1–3.4‰) at high tide and lower values (0–0.9‰) at low tide. As the river discharge increased from Initial to Rising, freshwater occupied Station E. This resulted in the fresh-saline water interface moving downstream, and the surface salinity at Station E decreased to 0‰, while the bottom salinity was lower than 0.1‰. As river runoff decreased, especially during the late falling and ending, the salinity at Station E recovered, and the fresh-brackish water interface moved back upstream. The water column remained oxic throughout the sampling period, although there was a distinct decrease in dissolved oxygen to approximately 2 mg L^{-1} during Rising period coincidental with the resuspension of surficial sediment from mudflats (Figure S1 in Supporting Information S1). pH and temperature showed minima at the same time as the salinity minima at Station E.

3.2. Temporal Variation in Suspended Particulate Matter

The surface SPM concentration at Station E varied with the bottom turbidity (Figures 3b and 3c). The SPM concentrations of Initial, Rising, Falling, and Ending were 129.4 ± 41.9, 185.9 ± 112.1, 174.5 ± 56.0, and 137.1 ± 49.2 mg L^{-1}, respectively. The bottom turbidity was 51.8 ± 26.9 NTU (Initial), 125.4 ± 96.5 NTU (Rising), 115.5 ± 50.8 (Falling), and 47.2 ± 26.1 NTU (Ending), respectively. There was a linear relationship between these two measurements (see inset in Figure 3c).

The daily SPM concentrations at the river outlets were 54.9 ± 30.8 mg L^{-1} for NJR and 38.6 ± 14.9 mg L^{-1} for WJR, for a total riverine concentration of 51.3 ± 16.4 mg L^{-1} (Figure 4a). The total riverine SPM flux

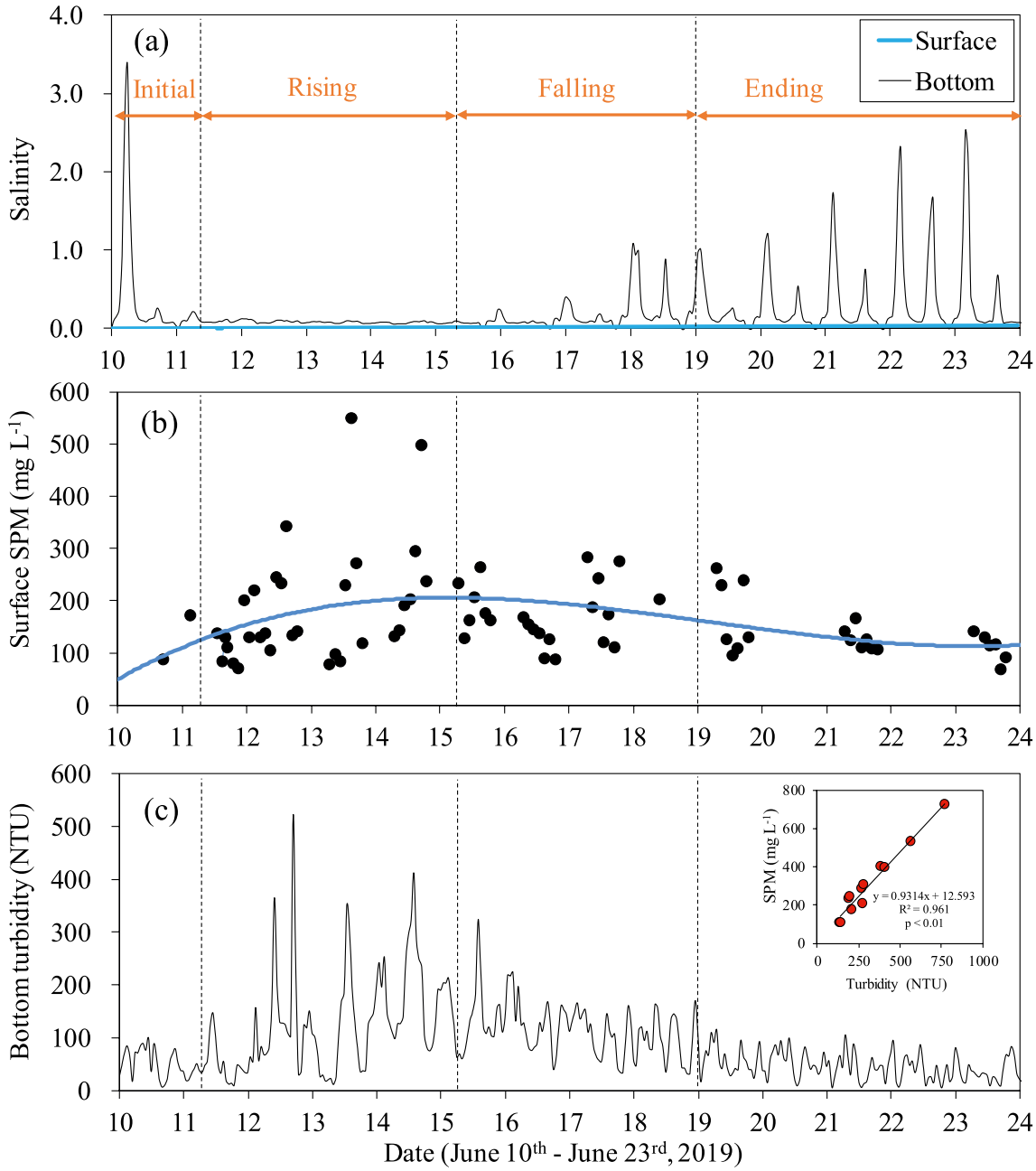

Figure 3. Comparison of (a) surface and bottom salinity, (b) surface SPM (mg L^{-1}) and (c) bottom turbidity (NTU) during the storm observation at Station E of the Jiulong River Estuary. Bottom salinity and turbidity were hourly results measured by in-situ multiparameter sonde (Aqua TROLL 600, USA). The inset in (c) shows the relationship between tubidity and SPM concentration on several samples where both were measured.

was 5,985 ± 5,048 t d^{-1}, of which 81.7 ± 7.5% was contributed by NJR and 18.3 ± 7.5% by WJR (Figure 4b). During baseflow, the SPM concentration and flux exported from the two tributaries were relatively stable. As discharge increased, riverine SPM concentration and flux increased sharply from 12 to 14 June, reaching a maximum of 97.6 mg L^{-1} and 17,745 t d^{-1}, respectively, and then decreased gradually back to the previous values (29.1 ± 5.1 mg L^{-1}, 2,440 ± 773 t d^{-1}) during the Ending period.

Riverine SPM concentration and flux composed a small proportion of SPM at Station E. During baseflow, the riverine SPM concentration and flux were only 23.5 ± 4.5% and 26.4 ± 5.3% of the values at Station E, respectively, while the contribution of riverine SPM concentration and flux to Station E increased to 39.0 ± 12.2% and 41.4 ± 15.3%, respectively, during flood. Therefore, most of the SPM at Station E came from the tidal river and

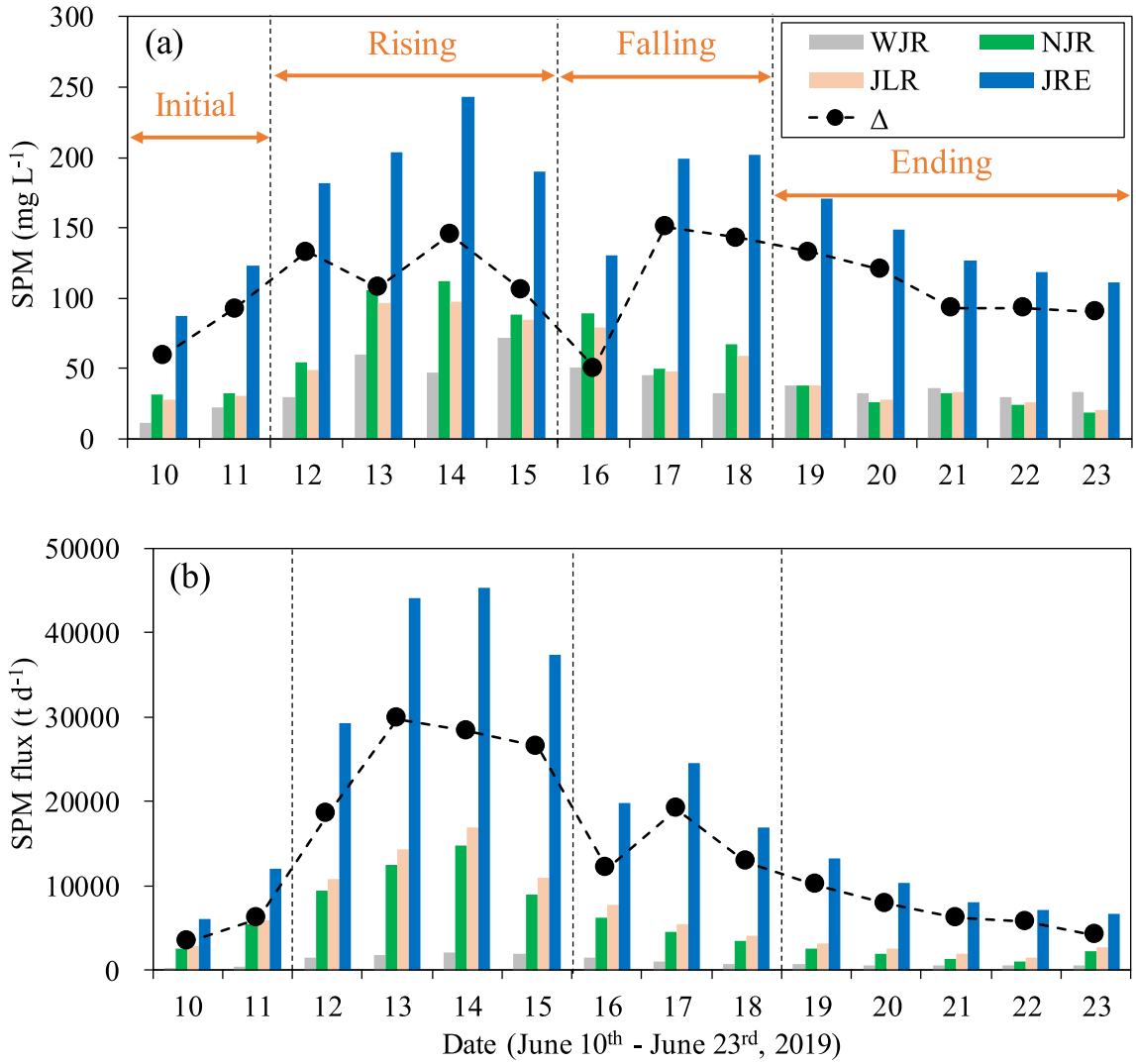

Figure 4. Daily concentration and flux of SPM at the outlets of the Jiulong River (ZS for WJR, JD for NJR) and comparison between the value of Station E (JRE) and river sum (JLR) during the storm observation. Δ (delta) indicated the difference between the value of Station E (JRE) and river sum (JLR), where a positive value meant concentration at Station E was higher than that of river sum.

upper estuary (Figure 4). At the beginning of Falling (16 June), the estuarine SPM concentration and flux, as well as those resuspended from the tidal river and upper estuary, both decreased gradually until the end of the sampling.

3.3. Evolution of Phosphorus Species Among River, Estuary and Tidal River

NJR and WJR both contributed riverine phosphorus to JRE. Comparatively, WJR had a similar TPP concentration (64.5 ± 17.1 μg P L^{-1}) to NJR (56.9 ± 22.8 μg P L^{-1}), while it had higher concentrations of DIP (70.2 ± 14.4 μg P L^{-1}) and DOP (102.0 ± 33.3 μg P L^{-1}) (Figure 5). With discharge more than three times higher than WJR (Figure 2b), NJR contributed considerably higher ($p < 0.01$) flux of TPP (5,138 ± 3,775 kg P d^{-1}) and DIP (2,975 ± 1,605 kg P d^{-1}) but lower flux of DOP (1,489 ± 1,421 kg P d^{-1}) (Figure 6). The riverine DOP concentration decreased on the first day of Rising (12 June) as discharge increased, and then it increased in the following part of Rising. The riverine flux of all phosphorus species increased with discharge and decreased from the last day of Rising (15 June) to the baseflow values.

The variation patterns of phosphorus concentration and flux at Station E were different from the riverine contributions (Figures 5 and 6). Both TPP concentration and flux at Station E increased from Initial to Rising, and

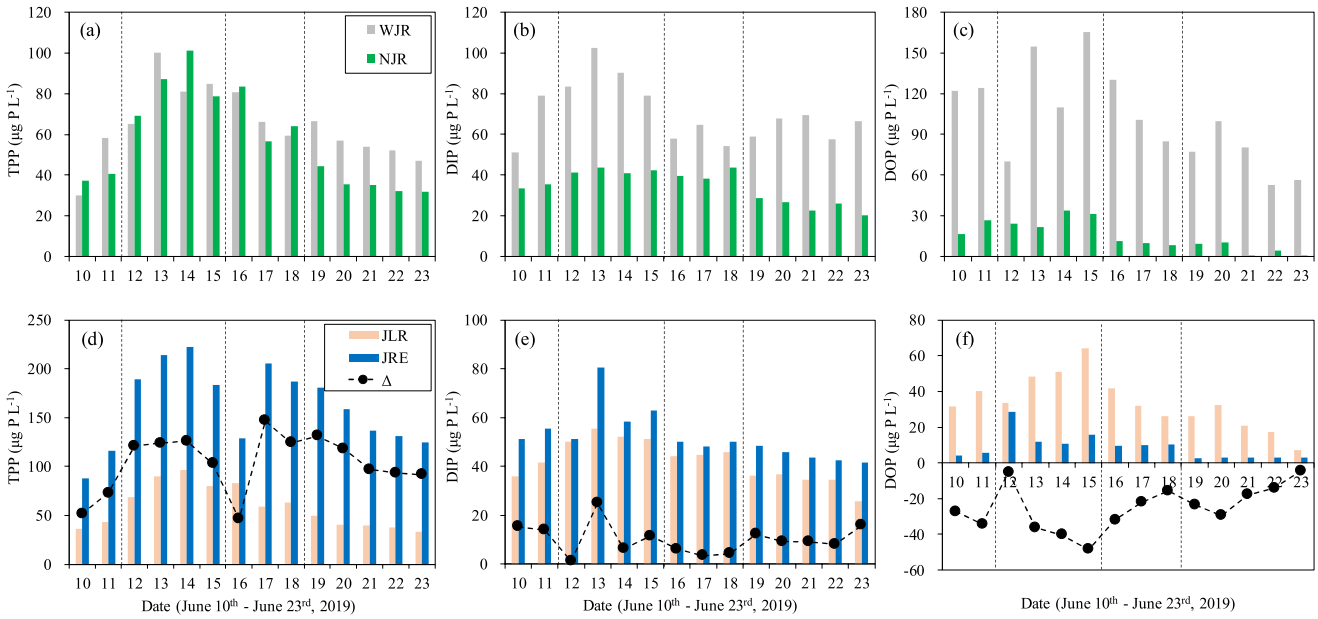

Figure 5. Daily concentration of (a) TPP, (b) DIP, and (c) DOP at the outlets of the Jiulong River (ZS for WJR, JD for NJR) and concentration comparison between Station E (JRE) and river sum (JLR) during the storm observation. Δ (delta) indicated the concentration difference between Station E (JRE) and river sum (JLR), where a positive value meant concentration at Station E was higher than that of river sum.

peaked in the middle of Rising before the maximum discharge. However, for the first day of Falling (16 June), the estuarine TPP sharply declined. Then, it recovered to a higher value on 17 June and gradually decreased. The DIP concentration at Station E was rather constant at approximately 40–60 μg P L^{-1}, except for a single higher value of 80 μg P L^{-1} on 13 June. Estuarine DOP reached its maximum concentration (28.4 μg P L^{-1}) and flux (2,447 kg P d^{-1}) on the first day of Rising (12 June), then it decreased rapidly and was only 2.9 ± 1.3 μg P L^{-1} and 155 ± 29 kg P d^{-1} in Ending.

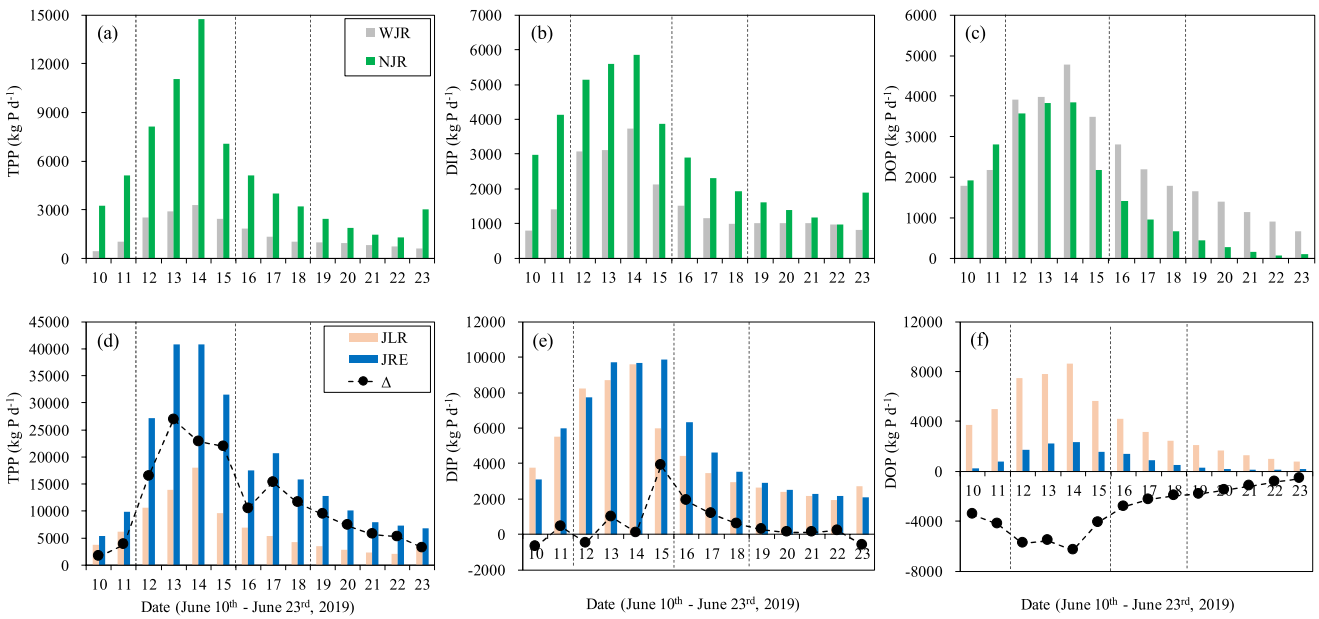

Figure 6. Daily flux of (a) TPP, (b) DIP, (c) DOP at the outlets of the Jiulong River (ZS for WJR, JD for NJR) and flux comparison between Station E (JRE) and river sum (JLR) during the storm observation. Δ (delta) indicated the flux difference between Station E (JRE) and river sum (JLR), where a positive value meant flux at Station E was higher than that of river sum.

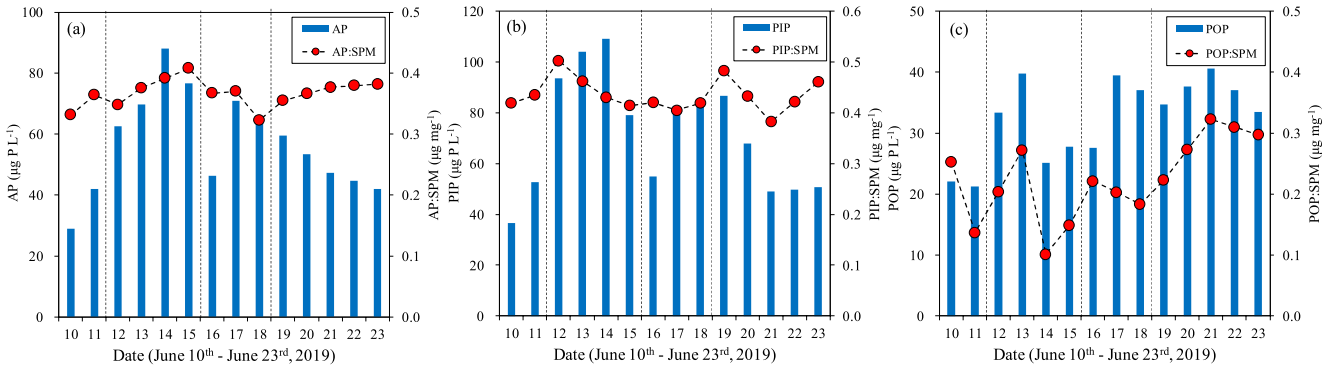

Figure 7. Daily concentration of particulate phosphorus species (AP, PIP, and POP) and their ratios to SPM at Station E (JRE) during the storm period (10 to 23 June 2019).

The differences (Δ) in phosphorus species between Station E and river outlets represented the contribution from the tidal river and the upper reaches of the Jiulong River Estuary. TPP and DIP showed considerable increases in concentration differences of 104.9 ± 30.6 and 10.1 ± 6.0 μg P L^{-1}, respectively (Figure 5), while DOP showed a decrease of −25.1 ± 12.4 μg P L^{-1}. The flux differences of TPP, DIP, and DOP were 11,568 ± 7,919, 582 ± 1,240, and −2,957 ± 2,097 kg P d^{-1}, respectively (Figure 6). The TPP difference increased during Rising period reaching a peak in the middle of Falling and then decreasing. The DIP concentration differences were much smaller than TPP and showed no obvious trend during the storm, apart from a single anomalous value on 12 June, Δ DOP showed increasingly negative values from Initial to the end of Rising followed by decreasingly negative values to Ending.

3.4. Structure and Adsorption Characteristics of Phosphorus at Station E

The proportion of particulate phosphorus at Station E was 70.4 ± 9.9%, which was always higher than that of the dissolved form, while the fraction of inorganic phosphorus (81.2 ± 8.3%) was also higher than that of organic P (Figure S6 in Supporting Information S1). The ratios of AP:SPM, PIP:SPM, and POP:SPM were 0.37 ± 0.02, 0.44 ± 0.03, and 0.26 ± 0.07 μg mg^{-1}, respectively (Figure 7). AP:SPM increased from the initial value (0.33 μg mg^{-1}) to the maximum value (0.41 μg mg^{-1}) at the end of Rising period, then it decreased continuously to the baseflow value (0.32 μg mg^{-1}) during Falling period and shift to increase during Ending period. PIP:SPM reached a maximum (0.50 μg mg^{-1}) at the beginning of Rising and remained stable during the Falling period with a minimum value (0.20 μg mg^{-1}).

3.5. Measurements of Parameters at Buoys in the Middle and Lower Jiulong River Estuary

A limited number of parameters were determined at two buoys in the middle and lower estuary (jy# and 3#) (Figure S7 in Supporting Information S1). The fluctuations in salinity at buoy jy# during baseflow were between 10 and 25‰ (tidally dependent) and decreased to 2–15‰ at the peak of flood. These values are typical of the middle of the estuary. At buoy 3#, the corresponding salinity fluctuations during the tidal cycle were higher, characteristic of an outer estuary station. The lowest salinity, which represents the peak discharge to the estuary, was on 15 June at buoy jy# but one day later at buoy 3#. Turbidity was lower in the middle estuary buoy than at Station E. DIP gradually increased in concentration at buoy 3# in the outer estuary, while chlorophyll *a* (Chl *a*) was highest at the beginning and end of the sampling period and lowest in the middle when turbidity at buoy jy# was highest.

4. Discussion

4.1. Sources of Phosphorus in the Jiulong River Catchment

Human activities are the main sources of phosphorus in the Jiulong River catchment (Zhang et al., 2018; Zhou et al., 2018). Anthropogenic phosphorus is discharged into the river channel through point sources and nonpoint sources (Yu et al., 2015). Yuan et al. (2021) found that a major source of anthropogenic P in the NJR was human

Table 1
Summary of Phosphorus Concentrations and Fluxes During the Storm at the River Outlets of the West River (WJR) and the North River (NJR)

Items	River	TP	TPP	DTP	DIP	DOP
EMC (μg P L^{-1})	WJR	251.7	69.4	182.4	74.5	107.9
	NJR	116.3	62.3	54.1	36.1	18.0
Baseflow (μg P L^{-1})	WJR	203.5	30.2	173.3	51.0	122.3
	NJR	86.9	37.1	49.8	33.4	16.4
P flux (kg P d^{-1})	WJR	5,495	1,514	3,981	1,626	2,355
	NJR	9,603	5,138	4,465	2,975	1,489

Note. EMC indicates event mean phosphorus concentration calculated as flow weighted mean concentration. Baseflow indicates the measured concentration at the start of the storm. P flux indicates the daily average phosphorus flux.

domestic waste and agricultural waste from intensive animal agriculture, which were discharged in the upper reaches of the river adjacent to Longyan city. As these polluted waters flowed downstream, the concentration of DIP decreased in part due to dilution by less polluted tributaries. In addition, part of the DIP was adsorbed onto inorganic particles as PIP, and part was converted into POP by biological growth, particularly in the cascade reservoirs that exist in the main channel (Lu et al., 2016; Maavara et al., 2015). During periods of relatively low flow, particulate P (PIP and POP) was retained in these cascade reservoirs in the surface sediment. In WJR, a major source of pollution in the upper reaches is intensive pomelo orchards (Lin et al., 2020; Yuan et al., 2021). These are intensively fertilized in winter, some of which is washed into the river channel, particularly during the wet season (Lin et al., 2020; Yuan et al., 2021). In addition, there are major inputs of treated domestic waste in Zhangzhou city, which is situated relatively near the outlet of WJR to the estuary. In addition, throughout the river catchment (both NJR and WJR), there are fewer sources of domestic and agricultural pollution, both point sources and nonpoint sources.

This anthropogenic P is transported down the Jiulong River to the estuary. The TPP concentration of NJR at the outlet was slightly higher than in WJR, while the DIP concentration in NJR was approximately 60% of the latter in June 2019 (Figures 5a and 5b). The P speciation of these chemical species measured at the same locations during normal wet season flow in July 2018 (Yuan et al., 2021) was broadly similar with the main differences being that there was higher TPP in WJR in July 2018 (80 vs. 30 μg P L^{-1}) and the difference between DIP in NJR and WJR was larger in July 2018 than in June 2019 (60 vs. 20 μg P L^{-1}). Such differences represent normal fluctuations in nutrient supply and removal in such inhomogeneous riverine systems. In the case of DOP, the main source of DOP in the river is treated domestic waste from Zhangzhou city (Table 1).

4.2. Effects of the Storm on Riverine Phosphorus

As has been found in previous studies in the Jiulong River and elsewhere, the effect of stormflow is to dramatically increase the flux and concentration of pollutant nutrients (both P and N) from the river catchment to the estuary (Aguilera & Melack, 2018; Blaen et al., 2017; Chen et al., 2015, 2018; Correll et al., 1999; Drewry et al., 2009). In this study, an entire storm was sampled (daily averages) through the Initial-Rising-Falling and Ending periods (10 to 23 June 2019). The catchment rainfall that led to this storm flood in the Jiulong River began from 9 June and ended in 13 June 2019, approximately 0.5–1 day earlier than the resulting flood pulses. Similar delays between rainfall and runoff formation have also been found in other studies (Chen et al., 2015).

Hysteresis effects were analyzed to unravel the export characteristics of phosphorus from the catchments during the storm. In NJR, TPP showed an anticlockwise trajectory around flood. There was a relatively simple linear increase in TPP (and SPM) in the NJR during Rising period as the increasing discharge caused progressively increased erosion of soil and sediment and washed preexisting TPP from pollutant sources such as human and animal waste from point sources (Figure 8a). Additionally, the TPP:SPM ratio decreased somewhat (Figure S4 in Supporting Information S1) from approximately 1.2 μg mg^{-1} during the Initial period to approximately 0.8 μg mg^{-1}. This change suggested that as the storm waters increased, there was both an increase in the highly polluted SPM from sewage treatment, agricultural sources and surficial sediments and an increase in relatively

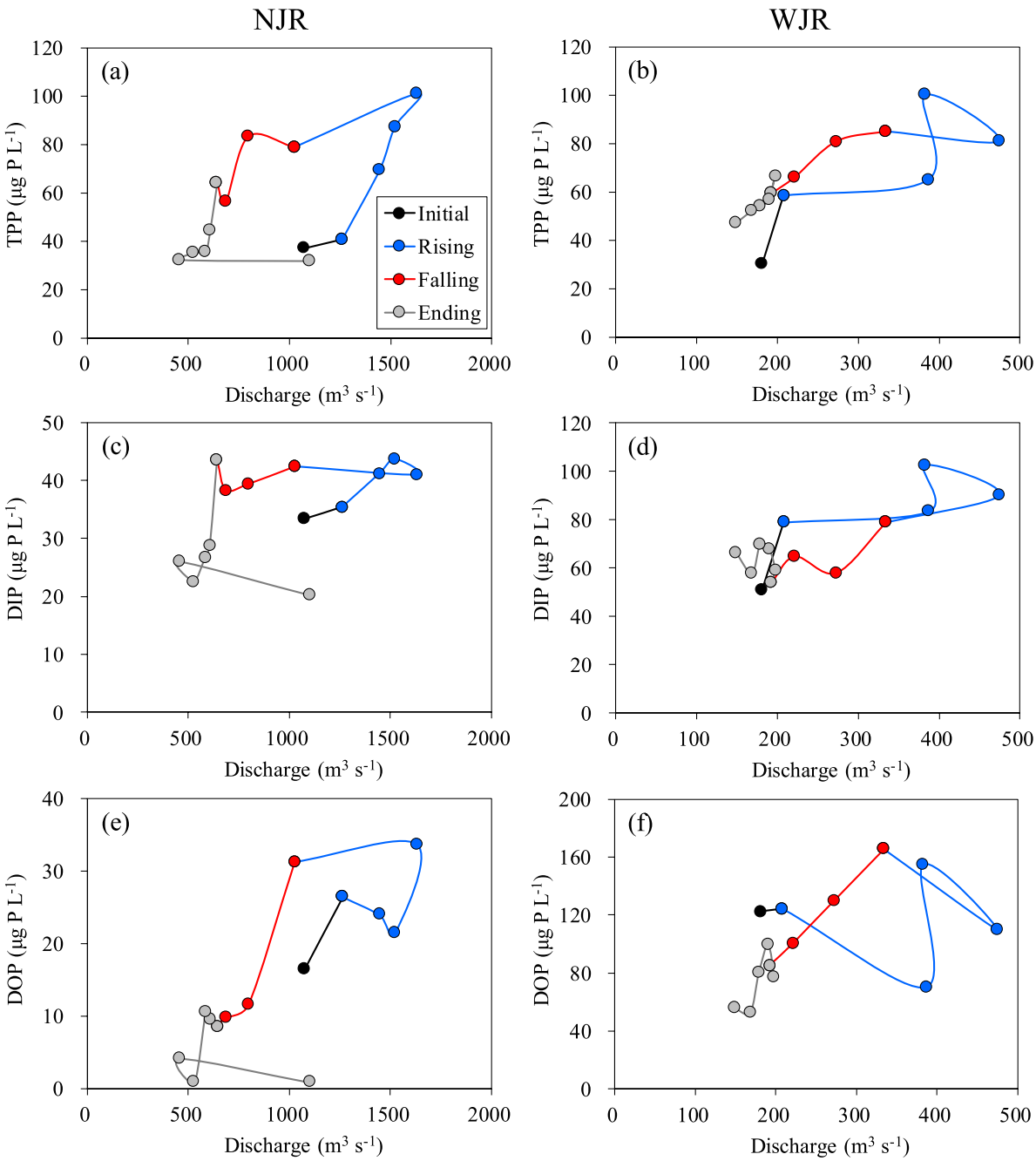

Figure 8. Relationship between daily phosphorus species (TPP, DIP and DOP) and the discharge at the river outlets in the West River (WJR) and the North River (NJR) during the storm observation period (10 to 23 June 2019).

less polluted soils eroded from river banks and fields that contained less P than the TPP present during the normal wet season flow (Yuan et al., 2021). There was a quasi-linear decrease in TPP during Falling period but at a higher level of TPP than during Rising period. This continued into the Ending period. Additionally, the TPP:SPM ratio gradually increased back to the initial values. This implied that the amount of diluting "soil-P" decreased more rapidly than the background high TPP particles as the discharge decreased and its erosive power lessened. The pattern in WJR was somewhat different in that there was a much smaller hysteresis effect.

The concentration of DIP in NJR was relatively closely matched to discharge, with only a small increase in concentration of 25% from 30 to 40 μg P L^{-1} during Rising period and an essentially constant concentration of

DIP during Falling period (Figure 5b). The pattern was similar to that determined by Chen et al. (2015) for three storms in 2013, but the concentration of DIP in this study (2019) was considerably less than the 50–150 μg P L^{-1} measured in 2013. It is, however, noted that AP increased rapidly at the beginning of Rising in the NJR (Figure S2a in Supporting Information S1), showing that a proportion of the increased SPM, likely the recently eroded soil/sediment, was not in equilibrium with the increased DIP and adsorbed some of the increased DIP. A parallel study (Lin et al., 2022) found that the ratio of NO_3-N to DIN in the NJR was more than 85%, confirming a strong agricultural signal during the storm.

Compared with the normal flow, the maximum flux of TPP, DIP, and DOP caused by the storm flood increased by 3.1, 0.8, and 2.1 times for NJR and 6.0, 3.6, and 1.4, times for WJR, respectively (Figure 6). Compared with previous storms (Chen et al., 2015) in the NJR, this storm event brings much lower phosphorus fluxes to the estuary (9,602 vs. 195,410 kg P d^{-1}). This was both because of the lower discharge (2,060 vs. 3,070 m^3 s^{-1}) as well as lower EMC (54 vs. 273 μg P L^{-1}) and because the 2019 storm was not the first flood event of the year resulting in a relatively smaller phosphorus output even though this storm had the longest duration in the year (Figure 2a).

4.3. Effects of the Storm on Estuarine Hydrological and Sedimentological Environments

A major effect of the increased storm water flow coming down the Jiulong River was on the location of the freshwater-brackish boundary and on the resuspension of previously deposited sediment from the upper estuary, as described in detail in Lin et al. (2022). The key changes and their implications for P geochemistry in the river-estuarine continuum are summarized here. The ETM during normal flow is located upstream of Station E in the vicinity of Stations A5-A7 (Yu et al., 2019). As the riverine flow increases during Rising period, this boundary moves downstream of Station E, which results in only freshwater (salinity = 0‰) at Station E and a relatively fast water flow. This increased the erosion capacity in the fetch upstream of Station E. As the flow decreased in Falling and Ending, the ETM moved back to the region of Station E.

During normal flow conditions, some of the sediment carried down the Jiulong River is deposited in the upper estuary. During the storm (Rising and Falling), the concentrations of SPM and TPP at Station E were considerably over and above the increase observed in the river. Similar increases have been observed previously (Chen et al., 2015). This increase is because of both increased sediment erosion and mobilization in the river catchment, including sediment flushing from the reservoirs behind dams in the NJR, by approximately 15,000 t d^{-1} and local resuspension in the upper estuary (approximately 28,000 t d^{-1}) as the ETM moved downstream (Figure 4).

The sediment that had been brought down and deposited in the upper estuary during periods of quiescent flow is characteristically high in labile organic matter and iron minerals (Pan, Guo, et al., 2019; Pan, Liu, et al., 2019). This was expected to result in characteristic changes in P geochemistry (Krom & Berner, 1981; Pan, Liu, et al., 2019), which are described in detail below. When these sediments were then resuspended, they not only increase the amount of SPM in the water column over and above that brought down the river, but also change the chemical species and the flux of P in the estuary and therefore flushed out of the estuary downstream.

Although the maximum turbidity (550 mg L^{-1}, Figure 3b) observed during the Rising period was much higher than that during normal flow, it was less than that in many previous storms. For example, the peak SPM during a storm in 2016 studied by Yu et al. (2019) was 1,500 mg L^{-1} at peak discharge. The nature and magnitude of peak SPM during storms depends on a number of different causes, including the maximum flow of water during that particular storm and how much sediment has been deposited in the upper estuary since it was last flushed out by a major storm. This storm in June 2019 was the second of three storms in summer, and the relatively small increase in SPM was due to previous flushing of the upper estuary in previous storms.

In addition to these major changes in SPM caused by river discharge, there were also changes related to the tide. Higher amounts of SPM are found during spring tide as a result of enhanced resuspension in stronger spring-tide currents (Yu et al., 2019). Diminishing tidal range during the storm observation led to a gradual decline in the amounts of resuspended particles from Falling to Ending (Figures 2c and 4).

4.4. Effects of the Storm on Estuarine Phosphorus

During the storm, there were higher TPP and DIP (though reduced DOP) concentrations measured at Station E over and above the extra supplied from the river catchment due to processes in the upper estuary (Figure 5). The

average TPP concentration was 118.4 ± 9.0 μg P L^{-1}, 1.5 times the riverine concentration (83.8 ± 10.6 μg P L^{-1}), which represented a maximum increase of approximately 25,000 kg P d^{-1} passing Station E at the peak of the storm (Figure 6d). It is known that during normal flow, SPM brought down the river, which is rich in labile organic matter and is deposited in the upper estuary and adjacent wetlands (Beusen et al., 2005). This process results in the removal of P (TPP and DIP), which is removed as P-rich sediment in the upper estuary (Sanders et al., 1997). A study (Pan, Liu, et al., 2019) conducted near Station E found that the TP concentration in surface mangrove sediment and intertidal zones is approximately 700 mg P kg^{-1}, higher than the average concentration in the Jiulong River (593 ± 60 mg P kg^{-1}) (Wang, 2015).

Once deposited in the upper estuary region, this fine-grained sediment then undergoes characteristic diagenetic reactions (Krom & Berner, 1981), with labile organic matter decomposing and oxygen in the pore waters being consumed. Typically, DIP is released both by microbial breakdown of organic matter containing phosphorus and by the release of DIP from iron-bound particles as Fe is reduced. These reactions are particularly intense in the warm temperatures of this subtropical estuary. A previous study (Pan et al., 2017) showed that the DIP concentration in the porewaters of mangrove sediments in the Jiulong River Estuary is approximately 82.0 ± 26.9 μg P L^{-1}, which is higher than the typical DIP in the overlying water (40–50 μg P L^{-1}) during baseflow.

It was observed that during the storm, the concentration and flux of TP (TPP + DIP + DOP; Figures 5 and 6) in the estuary increased considerably. Most of this increase was as TPP (50–150 μg P L^{-1}), with a much smaller increase in DIP (0–20 μg P L^{-1}) and a decrease in DOP (up to −50 μg P L^{-1}). The increased TPP in part reflects the observed increase in TPP in the surficial sediments, which were resuspended in the storm. However, although the flux of DIP increased considerably, particularly during the Rising phase of the storm, the concentration of DIP remained relatively constant at approximately 40 μg P L^{-1} (except for one datum on 13 June). It is characteristic of many turbid estuaries that the DIP concentration is buffered at a relatively low constant value (Froelich, 1988). Typically, this is due to the interaction between DIP and inorganic particles in the water column (Pan et al., 2013), as there is relatively little primary productivity because of the light limitation (Chen et al., 2018). In the Jiulong River Estuary during the Rising period, there was also a considerable increase in AP and PIP in the water column (both approximately 60 μg P L^{-1}), and the AP:SPM ratio increased during the Rising period by approximately 10%–15% (Figure 7). This provides direct evidence for the importance of increased inorganic adsorption of DIP onto the increased flux of particles in the estuary.

In this study, we suggested that the resuspended sediment represents an important locus for physical and microbial processes that remove DIP and DOP in the upper estuary. The decline in DO during Rising period was suggestive of oxidizing reactions taking place in the water column during the storm (Figure S1a in Supporting Information S1), such as the oxidation of reduced iron minerals to produce iron ferrihydrite. It is known that when Fe-rich anoxic sediment is exposed to increased oxygen, such as by resuspension into oxygen-rich overlying water, it forms Fe oxyhydroxides that are highly reactive to DIP (Krom & Berner, 1980, 1981; Niemisto & Lund-Hansen, 2019; Vaalama et al., 2019). In the case of the Jiulong River Estuary system, it is known that there is strong anoxic Fe reduction in the surface layers of mangrove sediments that are potentially available for resuspension (Lin, 2017; Pan, Guo, et al., 2019). Direct evidence in support of the removal of DIP onto particle surfaces was the increased AP:SPM ratio of particles at Rising of the storm (Figure S5d in Supporting Information S1). It has been shown that other microbial biogeochemical processes, such as nitrification, denitrification, and organic matter decomposition, take place in the water column of estuaries when anoxic sediments are resuspended (Niemistö et al., 2018). Direct evidence for such processes has been found as increased N microbial cycling processes during this storm in the Jiulong River Estuary (Lin et al., 2022). Currently, there are few studies on DOP mobilization and reactivity in estuarine waters, particularly during the nonsteady state conditions extant during storms (Brodlin et al., 2019). It was hypothesized that adsorption of DOP onto reactive mineral surfaces is a likely contributory cause for the decrease in DOP in the water column, although it is also possible that microbial processes that have been shown to be active in the water column at this time (e.g., denitrification and nitrification) (Lin et al., 2022) may also provide a sink for DOP (and maybe part of the DIP) during the peak of the storm.

As the storm decreased, with the exception of a single datum on 16 June, the TPP (and SPM) remained relatively high despite the input from the rivers decreasing considerably, with the TPP concentration during Falling period average of 146.7 ± 0.2 μg P L^{-1} (and SPM 146.9 ± 4.2 mg L^{-1}) and with a similar value of TPP:SPM ratio to that observed in the estuary throughout the storm (Figure S4 in Supporting Information S1). This change coincided with the freshwater-saline water boundary moving back to Station E and the ETM reestablishing itself at or close

Table 2
Weight Ratios of Total Dissolved Nitrogen (TDN) to Total Dissolved Phosphorus (TDP) (mean ± SD) at Each Stage of the Storm for the Summed Exit From the Rivers and for the Estuary (Station E)

Periods		Weight ratios of TDN:TDP (μg N:μg P)
Initial	WJR	42.7 ± 6.5
	NJR	42.8 ± 9.9
	JLR	42.6 ± 8.5
	JRE	58.3 ± 1.6
Rising	WJR	32.7 ± 5.1
	NJR	30.7 ± 5.4
	JLR	31.6 ± 4.4
	JRE	49.9 ± 5.8
Falling	WJR	42.3 ± 4.3
	NJR	34.3 ± 2.6
	JLR	38.0 ± 1.1
	JRE	60.9 ± 3.4
Ending	WJR	52.9 ± 8.7
	NJR	64.4 ± 11.7
	JLR	57.8 ± 8.7
	JRE	63.5 ± 11.3

Note. WJR indicates the West River, NJR indicates the North River, JLR indicates the river sum, and JRE indicates Station E in the Jiulong River Estuary.

to this location. As is characteristic of ETM's this means that there was local resuspension associated with the daily tidal cycle. However, these changes in the status of the estuary resulted in only approximately half of the TPP being fluxed out from the estuary during Falling period compared with the Rising (Figure S6 in Supporting Information S1).

4.5. Effects of Storms on the Outer Estuary and Implications for Coastal Integrated Management

In this study, TPP and TDP were not measured in the middle and outer estuary. However, a clear implication of this study is that bioavailable P (as both dissolved P and attached to particles) was mobilized during the storm and exported from the estuary to the coastal zone. In the estuary, when there were high levels of storm-related turbidity, the amount of additional algal growth was limited by light (Figure S7 in Supporting Information S1). However, as the storm effect subsided, the turbidity dropped out of the water column, and Chl *a* increased (Figure S7 in Supporting Information S1) (Chen et al., 2018). Such changes are typical of such systems, for example, De Carlo et al. (2007) found that there is a slow but steady increase in the phytoplankton standing stock over time in Kaneohe Bay after storm pulse input. Similar processes occur at locations where major rivers flow into lakes (Pearce et al., 2021), but such locations are not dominated by SPM and thus result in nutrient uptake by phytoplankton, including preferential P uptake and increased eutrophication in these lake estuaries.

Lin et al. (2022) determined the concentration and flux of N species in the river-estuary continuum for the same storm as has been studied in detail here for P species. It is therefore possible to determine the TDN:TDP ratio in the river-estuary continuum during the different phases of the storm. The ratio of TDN:TDP at each stage of the storm is shown in Table 2. During baseflow, the TDN:TDP (weight ratio) flowing out of the rivers was approximately 43:1 (μg N:μg P), which was much greater than the canonical Redfield weight ratio (7.2:1) for phytoplankton uptake and far greater than the N:P ratio of the fertilizers generally used in the Jiulong River catchment (Guo et al., 2011). According to Lin et al. (2020) and Yuan et al. (2021), the TDN:TDP of the major pollutant sources are approximately 118:1 (μg N:μg P) for the agricultural waste and approximately 35:1 (μg N:μg P) for the north urban waste discharged and reaching the river channel. In the Jiulong River system, the TDN:TDP ratio tends to increase as P is removed by inorganic adsorption in the river channel (Yuan et al., 2021). These processes combined resulted in a higher TDN:TDP ratio reaching the estuary (Table 2). Within the estuary during baseflow, there were additional processes that removed more DIP than TDN, resulting in an increased ratio of 58:1 (μg N:μg P). It is known that in the ETM of the Jiulong River Estuary, as with many other estuaries, DIP is removed from the water column by adsorption onto inorganic particles and subsequently is buffered at a relatively low constant value (Froelich, 1988).

During the storm, the total flux of both N and P from the river increased considerably relative to the baseflow. The total amount of TDN supplied (approximately 368,000 kg N d^{-1}) (Lin et al., 2022) from the rivers was relatively higher than the flux of TDP (approximately 11,300 kg P d^{-1}), and as a result, the TDN:TDP ratio decreased to 31-33:1 (μg N:μg P). As during baseflow, there was additional removal of DIP in the upper estuary, resulting in a TDN:TDP ratio of 50:1 (μg N:μg P), which we attributed to adsorption of DIP onto resuspended sediment particles rich in labile Fe oxyhydroxides (Krom & Berner, 1980). During Falling and Ending phases of the storm, the controls on TDN:TDP became more complex (and the ratios more variable) as there were interactions between processes of supply from different areas of the river catchments, dilution as the discharge decreased and biological and physical removal of dissolved phases in the river catchment and upper estuary as the ETM moved back upstream of Station E.

Xiamen Bay has been subject to increasing numbers of HABs, including occasional toxic red tides, over the past decade (Chen et al., 2021). They found that these blooms occurred dominantly during midsummer, which is the same time as the flushing of pollutant nutrients from the Jiulong River catchment by monsoonal storms as well

as by increased river flow (Chen et al., 2015; Lin et al., 2022; Yu et al., 2019; Yuan et al., 2021). This is also the period of increased nutrient supply from microbial respiration in coastal sediments due to higher temperatures. In addition, these diagenetic processes are likely to cause some limited recycling of the labile TPP brought down during storms and deposited as surficial sediment in the outer estuary and coastal areas during storms. It is considered that the increased flux of dissolved nutrients and the high N:P ratio during storms are important contributory factors to HABs in Xiamen Bay (Chen et al., 2021), as they have been found elsewhere (De Carlo et al., 2007; Qiu et al., 2019).

In summary, our study showed that estuaries represent locations for temporary deposition of labile TPP during normal flow. Major storms result in remobilization of particulate P. Processes in the upper estuary are dominated by interactions between P and the inorganic surface and by microbial respiration changes downstream in the estuary. We speculated that this particulate P was transported to the coastal zone, where it was partially remobilized. This together with the increased dissolved P that was fluxed through the estuary during storms, was likely to cause increased eutrophication in the P-limited outer estuary and coastal system.

Conflict of Interest

The authors declare no conflicts of interest relevant to this study.

Data Availability Statement

The data presented in this work can be found in the Supporting Information and can also be accessed at 4TU. Research Data (http://dx.doi.org/10.4121/20445024).

Acknowledgments
This research was supported by the National Natural Science Foundation of China (No. 41676098; 51961125203). The authors thank all the students who assisted with fieldwork and Junou Du for her technical assistance.

References

Aguilera, R., & Melack, J. M. (2018). Concentration-discharge responses to storm events in coastal California watersheds. *Water Resources Research*, *54*(1), 407–424. https://doi.org/10.1002/2017wr021578

Annamalai, H., & Liu, P. (2005). Response of the Asian summer monsoon to changes in El Nino properties. *Quarterly Journal of the Royal Meteorological Society*, *131*(607), 805–831. https://doi.org/10.1256/qj.04.08

Asmala, E., Carstensen, J., Conley, D. J., Slomp, C. P., Stadmark, J., & Voss, M. (2017). Efficiency of the coastal filter: Nitrogen and phosphorus removal in the Baltic Sea. *Limnology & Oceanography*, *62*, S222–S238. https://doi.org/10.1002/lno.10644

Beusen, A. H. W., Dekkers, A. L. M., Bouwman, A. F., Ludwig, W., & Harrison, J. (2005). Estimation of global river transport of sediments and associated particulate C, N, and P. *Global Biogeochemical Cycles*, *19*(4), GB4S05. https://doi.org/10.1029/2005gb002453

Blaen, P. J., Khamis, K., Lloyd, C., Comer-Warner, S., Ciocca, F., Thomas, R. M., et al. (2017). High-frequency monitoring of catchment nutrient exports reveals highly variable storm event responses and dynamic source zone activation. *Journal of Geophysical Research: Biogeosciences*, *122*(9), 2265–2281. https://doi.org/10.1002/2017jg003904

Bowes, M. J., House, W. A., Hodgkinson, R. A., & Leach, D. V. (2005). Phosphorus-discharge hysteresis during storm events along a river catchment: The River Swale, UK. *Water Research*, *39*(5), 751–762. https://doi.org/10.1016/j.watres.2004.11.027

Brodlin, D., Kaiser, K., Kessler, A., & Hagedom, F. (2019). Drying and rewetting foster phosphorus depletion of forest soils. *Soil Biology and Biochemistry*, *128*, 22–34. https://doi.org/10.1016/j.soilbio.2018.10.001

Burchard, H., Schuttelaars, H. M., & Ralston, D. K. (2018). Sediment trapping in estuaries. *Annual Review of Marine Science*, *10*(1), 371–395. https://doi.org/10.1146/annurev-marine-010816-060535

Canela, P., Clements, T. L. S., & Sobolev, D. (2020). High nitrogen to phosphorus ratio in a Texas coastal river: Origins and implications for nutrient pollution sources and exports. *Journal of Coastal Conservation*, *24*(4), 46–52. https://doi.org/10.1007/s11852-020-00765-5

Castagno, K. A., Jiménez-Robles, A. M., Donnelly, J. P., Wiberg, P. L., Fenster, M. S., & Fagherazzi, S. (2018). Intense storms increase the stability of tidal bays. *Geophysical Research Letters*, *45*(11), 5491–5500. https://doi.org/10.1029/2018GL078208

Chen, B. H., Wang, K., Dong, X., & Lin, H. (2021). Long-term changes in red tide outbreaks in Xiamen Bay in China from 1986 to 2017. *Estuarine, Coastal and Shelf Science*, *249*, 107095–107101. https://doi.org/10.1016/j.ecss.2020.107095

Chen, N. W., Krom, M. D., Wu, Y. Q., Yu, D., & Hong, H. S. (2018). Storm induced estuarine turbidity maxima and controls on nutrient fluxes across river-estuary-coast continuum. *Science of the Total Environment*, *628–629*, 1108–1120. https://doi.org/10.1016/j.scitotenv.2018.02.060

Chen, N. W., Wu, Y. Q., Chen, Z. H., & Hong, H. S. (2015). Phosphorus export during storm events from a human perturbed watershed, southeast China: Implications for coastal ecology. *Estuarine, Coastal and Shelf Science*, *166*, 178–188. https://doi.org/10.1016/j.ecss.2015.03.023

Chen, Y. C., Liu, J. H., Kuo, J. T., & Lin, C. F. (2013). Estimation of phosphorus flux in rivers during flooding. *Environmental Monitoring and Assessment*, *185*(7), 5653–5672. https://doi.org/10.1007/s10661-012-2974-5

Conley, D. J., Smith, W. M., Cornwell, J. C., & Fisher, T. R. (1995). Transformation of particle-bound phosphorus at the land-sea interface. *Estuarine, Coastal and Shelf Science*, *40*(2), 161–176. https://doi.org/10.1016/S0272-7714(05)80003-4

Correll, D. L., Jordan, T. E., & Weller, D. E. (1999). Transport of nitrogen and phosphorus from Rhode River watersheds during storm events. *Water Resources Research*, *35*(8), 2513–2521. https://doi.org/10.1029/1999wr900058

De Carlo, E. H., Hoover, D. J., Young, C. W., Hoover, R. S., & Mackenzie, F. T. (2007). Impact of storm runoff from tropical watersheds on coastal water quality and productivity. *Applied Geochemistry*, *22*(8), 1777–1797. https://doi.org/10.1016/j.apgeochem.2007.03.034

Drewry, J. J., Newham, L. T., & Croke, B. F. (2009). Suspended sediment, nitrogen and phosphorus concentrations and exports during storm-events to the Tuross Estuary, Australia. *Journal of Environmental Management*, *90*(2), 879–887. https://doi.org/10.1016/j.jenvman.2008.02.004

Elser, J. J., Andersen, T., Baron, J. S., Bergström, A. K., Jansson, M., Kyle, M., et al. (2009). Shifts in lake N:P stoichiometry and nutrient limitation driven by atmospheric nitrogen deposition. *Science*, *326*(5954), 835–837. https://doi.org/10.1126/science.1176199

Fernandes, L., & Nayak, G. N. (2009). Distribution of sediment parameters and depositional environment of mudflats of Mandovi Estuary, Goa, India. *Journal of Coastal Research*, *2009*(252), 273–284. https://doi.org/10.2112/05-0614.1

Froelich, P. N. (1988). Kinetic control of dissolved phosphate in natural rivers and estuaries: A primer on the phosphate buffer mechanism. *Limnology & Oceanography*, *33*(4part2), 649–668. https://doi.org/10.4319/lo.1988.33.4part2.0649

Garnier, J., Billen, G., Nemery, J., & Sebilo, M. (2010). Transformations of nutrients (N, P, Si) in the turbidity maximum zone of the Seine Estuary and export to the sea. *Estuarine, Coastal and Shelf Science*, *90*(3), 129–141. https://doi.org/10.1016/j.ecss.2010.07.012

Guo, Z., Yuan, H. F., Zhang, X., Song, C. F., Li, X. Y., & Xie, J. C. (2011). A new approach to rapid determination of compound fertilizer composition. *Spectroscopy and Spectral Analysis*, *31*(9), 2424–2427. https://doi.org/10.3964/j.issn.1000-0593(2011)09-2424-04

Hong, H. S., Chen, N. W., & Wang, D. L. (2015). River-estuary-coast continuum: Biogeochemistry and ecological response to increasing human and climatic changes - Editorial overview. *Estuarine, Coastal and Shelf Science*, *166*, 144–145. https://doi.org/10.1016/j.ecss.2015.10.036

Hu, M. J., Sardans, J., Le, Y. X., Wang, Y. F., Penuelas, J., & Tong, C. (2021). Phosphorus mobilization and availability across the freshwater to oligohaline water transition in subtropical estuarine marshes. *Catena*, *201*, 105195–105205. https://doi.org/10.1016/j.catena.2021.105195

Huang, J. L., & Hong, H. S. (2010). Comparative study of two models to simulate diffuse nitrogen and phosphorus pollution in a medium-sized watershed, southeast China. *Estuarine, Coastal and Shelf Science*, *86*(3), 387–394. https://doi.org/10.1016/j.ecss.2009.04.003

Huang, Y. L., Tang, L., Huang, J. L., & Xiao, C. R. (2019). Responses of riverine phosphorus exports to land use and hydrological regime in the Jiulong River Watershed. *Huanjing Kexue*, *40*(12), 5340–5347. https://doi.org/10.13227/j.hjkx.201905234

Krom, M. D., & Berner, R. A. (1980). Adsorption of phosphate in anoxic marine sediments. *Limnology & Oceanography*, *25*(5), 797–806. https://doi.org/10.4319/lo.1980.25.5.0797

Krom, M. D., & Berner, R. A. (1981). The diagenesis of phosphorus in a nearshore marine sediment. *Geochimica et Cosmochimica Acta*, *45*(2), 207–216. https://doi.org/10.1016/0016-7037(81)90164-2

Li, L. G., He, Z. L., Li, Z. G., Li, S. L., Wan, Y. S., & Stoffella, P. J. (2017). Spatiotemporal change of phosphorous speciation and concentration in stormwater in the St. Lucie Estuary watershed, South Florida. *Chemosphere*, *172*, 488–495. https://doi.org/10.1016/j.chemosphere.2017.01.020

Lin, C. Q. (2017). *Distribution characteristics and source analysis of trace elements in offshore surface sediments from the Jiulong River (In Chinese) (Master thesis)*. Huaqiao University.

Lin, J. J., Chen, N. W., Yuan, X., Tian, Q., Hu, A. Y., & Zheng, Y. (2020). Impacts of human disturbance on the biogeochemical nitrogen cycle in a subtropical river system revealed by nitrifier and denitrifier genes. *Science of the Total Environment*, *746*, 141139–141150. https://doi.org/10.1016/j.scitotenv.2020.141139

Lin, J. J., Krom, M. D., Wang, F. F., Cheng, P., Yu, Q. B., & Chen, N. W. (2022). Simultaneous observations revealed the non-steady state effects of a tropical storm on the export of particles and inorganic nitrogen through a river-estuary continuum. *Journal of Hydrology*, *606*, 127438–127450. https://doi.org/10.1016/j.jhydrol.2022.127438

Lu, T., Chen, N. W., Duan, S. W., Chen, Z. H., & Huang, B. Q. (2016). Hydrological controls on cascade reservoirs regulating phosphorus retention and downriver fluxes. *Environmental Science and Pollution Research*, *23*(23), 24166–24177. https://doi.org/10.1007/s11356-016-7397-3

Maavara, T., Parsons, C. T., Ridenour, C., Stojanovic, S., Duerr, H. H., Powley, H. R., & Van Cappellen, P. (2015). Global phosphorus retention by river damming. *Proceedings of the National Academy of Sciences of the United States of America*, *112*(51), 15603–15608. https://doi.org/10.1073/pnas.1511797112

Nelson, C. R. B. (2000). The biogeochemical cycling of phosphorus in marine systems. *Earth-Science Reviews*, *51*(1–4), 109–135. https://doi.org/10.1016/s0012-8252(00)00018-0

Niemistö, J., Kononets, M., Ekeroth, N., Tallberg, P., Tengberg, A., & Hall, P. O. J. (2018). Benthic fluxes of oxygen and inorganic nutrients in the archipelago of Gulf of Finland, Baltic Sea – Effects of sediment resuspension measured in situ. *Journal of Sea Research*, *135*, 95–106. https://doi.org/10.1016/j.seares.2018.02.006

Niemisto, J., & Lund-Hansen, L. C. (2019). Instantaneous effects of sediment resuspension on inorganic and organic Benthic nutrient fluxes at a shallow water coastal site in the Gulf of Finland, Baltic Sea. *Estuaries and Coasts*, *42*(8), 2054–2071. https://doi.org/10.1007/s12237-019-00648-5

Pan, F., Guo, Z. R., Cai, Y., Liu, H. T., Wu, J. Y., Fu, Y. Y., et al. (2019). Kinetic exchange of remobilized phosphorus related to phosphorus-iron-sulfur biogeochemical coupling in coastal sediment. *Water Resources Research*, *55*(12), 10494–10517. https://doi.org/10.1029/2019WR025941

Pan, F., Liu, H. T., Guo, Z. R., Li, Z. W., Wang, B., Cai, Y., & Gao, A. G. (2019). Effects of tide and season changes on the iron-sulfur-phosphorus biogeochemistry in sediment porewater of a mangrove coast. *Journal of Hydrology*, *568*, 686–702. https://doi.org/10.1016/j.jhydrol.2018.11.002

Pan, F., Liu, H. T., Guo, Z. R., Li, Z. W., Wang, B., & Gao, A. G. (2017). Geochemical behavior of phosphorus and iron in porewater in a mangrove tidal flat and associated phosphorus input into the ocean. *Continental Shelf Research*, *150*, 65–75. https://doi.org/10.1016/j.csr.2017.09.012

Pan, G., Krom, M. D., Zhang, M. Y., Zhang, X. W., Wang, L. J., Dai, L. C., et al. (2013). Impact of suspended inorganic particles on phosphorus cycling in the Yellow River (China). *Environmental Science & Technology*, *47*(17), 9685–9692. https://doi.org/10.1021/es4005619

Pearce, N. J. T., Larson, J. H., Evans, M. A., Frost, P. C., & Xenopoulos, M. A. (2021). Episodic nutrient addition affects water column nutrient processing rates in river-to-lake transitional zones. *Journal of Geophysical Research: Biogeosciences*, *126*(11), e2021JG006374. https://doi.org/10.1029/2021JG006374

Powers, S. M., Bruulsema, T. W., Burt, T. P., Chan, N. I., Elser, J. J., Haygarth, P. M., et al. (2016). Long-term accumulation and transport of anthropogenic phosphorus in three river basins. *Nature Geoscience*, *9*(5), 353–356. https://doi.org/10.1038/ngeo2693

Qiu, D. J., Zhong, Y., Chen, Y. Q., Tan, Y. H., Song, X. Y., & Huang, L. M. (2019). Short-term phytoplankton dynamics during typhoon season in and near the Pearl River Estuary, South China Sea. *Journal of Geophysical Research: Biogeosciences*, *124*(2), 274–292. https://doi.org/10.1029/2018JG004672

Reinhard, C. T., Planavsky, N. J., Gill, B. C., Ozaki, K., Robbins, L. J., Lyons, T. W., et al. (2017). Evolution of the global phosphorus cycle. *Nature*, *541*(7637), 386–389. https://doi.org/10.1038/nature20772

Rozemeijer, J., Noordhuis, R., Ouwerkerk, K., Dionisio Pires, M., Blauw, A., Hooijboer, A., & Van Oldenborgh, G. J. (2021). Climate variability effects on eutrophication of groundwater, lakes, rivers, and coastal waters in the Netherlands. *Science of the Total Environment*, *771*, 145366. https://doi.org/10.1016/j.scitotenv.2021.145366

Ryther, J. H. (1954). The ecology of phytoplankton blooms in Moriches Bay and Great south Bay, Long Island, New York. *The Biological Bulletin*, *106*(2), 198–209. https://doi.org/10.2307/1538713

Sanders, R. J., Jickells, T., Malcolm, S., Brown, J., Kirkwood, D., Reeve, A., et al. (1997). Nutrient fluxes through the Humber estuary. *Journal of Sea Research*, *37*(1), 3–23. https://doi.org/10.1016/S1385-1101(96)00002-0

Seitzinger, S. P., Mayorga, E., Bouwman, A. F., Kroeze, C., Beusen, A. H. W., Billen, G., et al. (2010). Global river nutrient export: A scenario analysis of past and future trends. *Global Biogeochemical Cycles*, *24*, GB0A08. https://doi.org/10.1029/2009gb003587

Slomp, C. P. (2011). Phosphorus cycling in the estuarine and coastal zones. In E. Wolanski & D. McClusky (Eds.), *Treatise on estuarine and coastal science* (pp. 201–229). https://doi.org/10.1016/B978-0-12-374711-2.00506-4

Vaalama, A., Hartikainen, H., Vallius, H., & Lukkari, K. (2019). Phosphorus exchange in eutrophied coastal brackish water sediments-sorption pattern, potential and factors affecting them. *SN Applied Sciences*, *1*(11). https://doi.org/10.1007/s42452-019-1374-7

Wang, S. (2015). *Study on nutrient pollution in surface sediments of Jiulong River Basin (In Chinese) (Master thesis)*. Huaqiao University.

Wu, M. F., Yang, F. X., Yao, Q. Z., Bouwman, L., & Wang, P. P. (2020). Storm-induced sediment resuspension in the Changjiang River Estuary leads to alleviation of phosphorus limitation. *Marine Pollution Bulletin*, *160*, 111628–111636. https://doi.org/10.1016/j.marpolbul.2020.111628

Xenopoulos, M. A., Downing, J. A., Kumar, M. D., Menden-Deuer, S., & Voss, M. (2017). Headwaters to oceans: Ecological and biogeochemical contrasts across the aquatic continuum. *Limnology & Oceanography*, *62*, S3–S14. https://doi.org/10.1002/lno.10721

Xu, J., Yin, K. D., He, L., Yuan, X. C., Ho, A. Y. T., & Harrison, P. J. (2008). Phosphorus limitation in the northern south China sea during late summer: Influence of the Pearl River. *Deep Sea Research Part I: Oceanographic Research Papers*, *55*(10), 1330–1342. https://doi.org/10.1016/j.dsr.2008.05.007

Yang, Y. Y., Asal, S., & Toor, G. S. (2021). Residential catchments to coastal waters: Forms, fluxes, and mechanisms of phosphorus transport. *Science of the Total Environment*, *765*, 142767–142778. https://doi.org/10.1016/j.scitotenv.2020.142767

Yu, D., Chen, N. W., Cheng, P., Yu, F. L., & Hong, H. S. (2020). Hydrodynamic impacts on tidal-scale dissolved inorganic nitrogen cycling and export across the estuarine turbidity maxima to coast. *Biogeochemistry*, *151*, 81–98. https://doi.org/10.1007/s10533-020-00712-4

Yu, D., Chen, N. W., Krom, M. D., Lin, J. J., Cheng, P., Yu, F. L., et al. (2019). Understanding how estuarine hydrology controls ammonium and other inorganic nitrogen concentrations and fluxes through the subtropical Jiulong River Estuary, S.E. China under baseflow and flood-affected conditions. *Biogeochemistry*, *142*(3), 443–466. https://doi.org/10.1007/s10533-019-00546-9

Yu, D., Yan, W. J., Chen, N. W., Peng, B. R., Hong, H. S., & Zhuo, G. H. (2015). Modeling increased riverine nitrogen export: Source tracking and integrated watershed-coast management. *Marine Pollution Bulletin*, *101*(2), 642–652. https://doi.org/10.1016/j.marpolbul.2015.10.035

Yuan, X., Krom, M. D., Zhang, M. Z., & Chen, N. W. (2021). Human disturbance on phosphorus sources, processes and riverine export in a subtropical watershed. *Science of the Total Environment*, *769*, 144658–144671. https://doi.org/10.1016/j.scitotenv.2020.144658

Zhang, X., Zhou, L., & Liu, Y. Q. (2018). Modeling land use changes and their impacts on non-point source pollution in a southeast China coastal watershed. *International Journal of Environmental Research and Public Health*, *15*(8), 1593–1607. https://doi.org/10.3390/ijerph15081593

Zhou, P., Huang, J. L., & Hong, H. S. (2018). Modeling nutrient sources, transport and management strategies in a coastal watershed, Southeast China. *Science of the Total Environment*, *610*, 1298–1309. https://doi.org/10.1016/j.scitotenv.2017.08.113